Structural changes in silver bromide at the melting point

1992 J. Phys.: Condens. Matter 4 6703

(http://iopscience.iop.org/0953-8984/4/32/005)

J. Phys.: Condens. Matter 4 (1992) 6703–6714. Printed in the UK

Structural changes in silver bromide at the melting point

V M Nield†, D A Keen‡, W Hayes† and R L McGreevy†

† Department of Physics, Clarendon Laboratory, Parks Road, Oxford OX1 3PU, UK
‡ ISIS Science Division, Rutherford Appleton Laboratory, Chilton, Didcot, Oxon OX11 0QX, UK

Received 10 April 1992, in final form 8 June 1992

Abstract. A neutron diffraction study has been performed on AgBr at a series of temperatures from 293 K to 706 K (melting point, T_m = 701 K), including measurements as close as 0.3±0.05° from T_m. Analysis of the structure factors using the reverse Monte Carlo modelling technique indicates that the motion of the Ag^+ ions about their rocksalt lattice sites is anisotropic, with increasing occupancy of the $(\frac{1}{4}\frac{1}{4}\frac{1}{4})$ tetrahedral interstitial site as the melting point is approached. It is concluded that the silver sub-lattice is undergoing a second-order transition to a fast-ion phase in which both tetrahedral and octahedral sites are occupied (possibly similar to the fast-ion transition in the high pressure FCC phase of AgI) although melting prevents complete transition. There is a clear discontinuity in Bragg scattering at T_m, suggesting that the first-order nature of the melting transition is unaffected.

1. Introduction

Silver bromide has been studied extensively because of its use in the photographic process (see Hamilton (1988) for a detailed review) and its chemical similarity to the fast-ion conductor silver iodide. However, these two compounds have different structures at ambient temperature and pressure, reflecting the increasingly covalent nature of the bonding as one goes from bromide to iodide. Silver iodide is stable at low temperatures and normal pressures in the hexagonal wurtzite structure and metastable in the cubic sphalerite (zinc-blende) structure. At 420 K it undergoes a structural phase transition to the fast-ion conducting α-phase, where the iodide ions vibrate about BCC lattice sites, surrounded by highly mobile silver ions which preferentially occupy the tetrahedral voids (Boyce *et al* 1977). At ambient temperature and increased pressure (greater than about 4 kbar) AgI exists in the face-centered cubic (FCC) (rocksalt) structure (Mellander *et al* 1980, Akella *et al* 1969). In this phase ionic conductivity measurements suggest a diffuse order–disorder transition to fast-ion behaviour as the temperature increases (Mellander 1982, Tallon and Buckley 1983). AgBr occurs in the rocksalt structure right up to the melting point at atmospheric pressure and has not been reported to have a fast-ion transition. In spite of this, the ionic conductivity at the melting point is only a factor of three less than that of α-AgI ($\sigma_{T_m}(\mathrm{AgBr}) \simeq 1\,\Omega^{-1}\mathrm{cm}^{-1}$, $\sigma_{T_m}(\mathrm{AgI}) = 2.6\,\Omega^{-1}\mathrm{cm}^{-1}$).

The predominant thermally induced defect in AgBr, as determined by transport and thermal expansion measurements, is the cation Frenkel interstitial (Lawn 1963), although a temperature independent Frenkel energy could not explain the rapid

0953-8984/92/326703+12$04.50

increase in ionic conductivity starting 150° below melting (Devlin and Corish 1987). The large number of such defects indicates the possibility of a transition to fast-ion conducting behaviour. However, it has been suggested that the increasing number of anion Schottky defects produces a lattice instability which precipitates melting before a second-order fast-ion transition occurs (Andreoni and Tosi 1983).

In two previous papers (Keen *et al* 1990a,b—hereafter referred to as I and II, respectively) we have reported the results of a neutron diffraction study of AgBr, where reverse Monte Carlo (RMC) modelling (McGreevy and Pusztai 1988) was used to draw detailed structural conclusions. In particular, information about the temperature dependences of interstitial occupancy and conductivity pathways was deduced. In this paper the previous data (I and II) have been re-analysed by RMC modelling of structure factors, as opposed to radial distribution functions; the truncation problem which previously made treatment of the low temperature data sets unsatisfactory has thus been removed. This extension of the RMC technique to model structure factor data containing sharp features is described. We examine in detail the relative positions of Ag^+ and Br^- to try and elucidate whether the increasing disorder prior to melting is indicative of 'pre-melting', or whether it is indeed a precursor of a second-order fast-ion transition which never reaches completion. New powder diffraction measurements taken within 0.3° of the melting point are reported.

2. Experimental details

The measurement and correction of powder neutron diffraction data, from AgBr at 293, 490, 669, 684, 689, 697, 698, and 699±2 K and of diffraction data from the liquid at 703 and 706±2 K, (the melting point is 701 K) have been described elsewhere (II). The structure factors measured from the powder include both Bragg and diffuse scattering, but obviously there is no Bragg scattering from the liquid. For measurements even closer to T_m a high-precision furnace arrangement (figure 1) has been developed to ensure small temperature fluctuations and high stability over long periods. This consists of a massive nickel block (large heat capacity) with a cut-out to allow the passage of neutrons, the cut-out being lined with neutron absorbing gadolinium foil to decrease multiple scattering. Temperature gradients across the sample are reduced by surrounding the sample position by a vanadium heat shield. Heating is by means of two resistive cartridge heaters, symmetrically placed in the top and bottom of the block. The temperature is measured by a platinum resistance thermometer connected to a six-decade resistance bridge which is computer controlled. The deviation from the set point is used to drive a standard proportional integral differential (PID) feedback system, with long time constants for stability. The furnace may be operated in isolation (up to about 600 K) or it may be inserted inside a neutron scattering furnace with standard control and heating. In this experiment the external heating element was a very thin tantalum cylinder through which a high current was passed. This provided the bulk of the heating, while the fine temperature control was maintained by the high precision insert. A stability of better than 50 mK at $\sim$ 1000 K can be maintained for several days using this arrangement, the limit being set by electrical noise from the external furnace controller.

New powder neutron diffraction measurements of AgBr were made at temperatures 1.4, 1.1, 0.6 and 0.3±0.05° below T_m on the D20 diffractometer at the Institut Laue-Langevin, again including both Bragg and diffuse scattering. The height of the

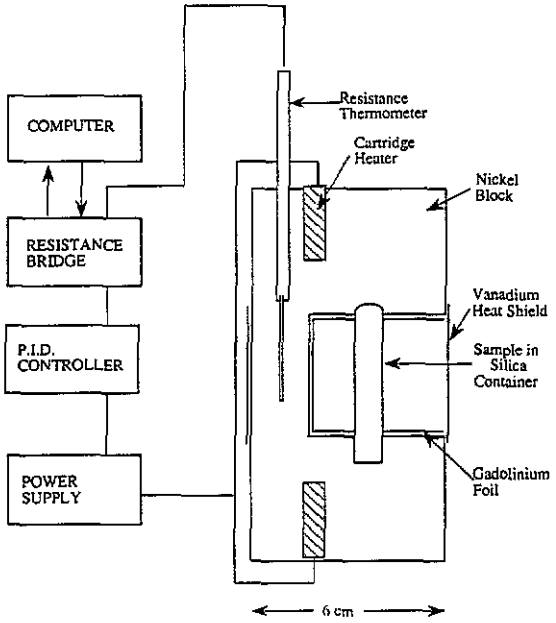

Figure 1. Furnace insert, used to obtain high precision and stability for measurements close to the melting point.

(200) Bragg peak was also measured continuously at one minute intervals during slow heating. Sample dependent scattering from the external furnace heat shields, and poor alignment of soller slits placed in front of the linear multi-detector to minimize this scattering, resulted in an angle dependent detector efficiency. We could not accurately correct for this and so the resultant structure factors contain a modulation. However, comparison of these structure factors indicates that little change is occurring in diffuse scattering in this temperature region. The radial distribution function obtained by Fourier transformation of the structure factor closest to T_m was very similar to that of the previous highest temperature measurement of the solid (see figure 2); a detailed comparison is impossible since it is not obvious how the structure factor modulations affect the real-space distribution, but the differences between the two are probably within the errors. The four new data sets are so similar that it is unnecessary to show them all.

3. Analysis

In standard crystallographic methods of analysis only the (elastic) Bragg scattering is used. This is determined by the time average structure of the system. If the time average structure deviates from the instantaneous structure then the intensities of the Bragg peaks decrease at high Q and scattering appears between Bragg peaks. This is (thermal) diffuse scattering. Diffuse scattering may also be produced by static disorder in the structure. As the level of disorder increases with temperature the number of resolvable Bragg peaks decreases and the number of parameters required to reproduce the effects of anharmonicity and anisotropy increases; the problem

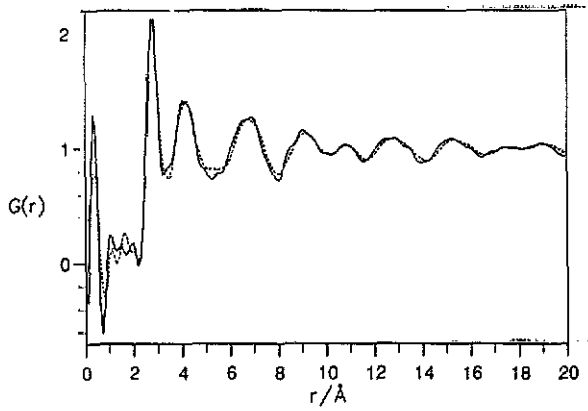

Figure 2. Radial distribution functions, $g_E(r)$, for AgBr. The new highest temperature data at 700.7 K is shown by the solid line and the previous measurement at 699 K by the dashed line.

becomes poorly determined. In any case the elastic scattering, being related to a time average, does not provide information on the instantaneous local atomic correlations (though these may be imposed by the particular model used to fit the data). This information, which is of interest in the study of disorder, is provided by the total, i.e. energy integrated, scattering, that is both Bragg and diffuse scattering.

The total structure factors for AgBr have been analysed using the reverse Monte Carlo (RMC) modelling technique, described in I and II and in greater detail by McGreevy *et al* (1990). The technique is similar to Metropolis Monte Carlo modelling (Metropolis *et al* 1953), except that one moves atoms to minimize the difference between the measured and calculated structure factors, rather than to minimize the energy. Therefore no potential is required. One disadvantage of the method is that it will tend to produce the most disordered structure consistent with the data, and this must be remembered when interpreting the results.

In order to model a crystalline material successfully using this method, care must be taken in the treatment of the Bragg peaks. This is because Bragg peaks represent long (essentially infinite) range order and therefore cannot be simulated in a finite-sized configuration, the maximum number of atoms being dictated by CPU time considerations. In the initial study (I, II) this problem was circumvented by fitting to the radial distribution function (obtained by Fourier transformation of the structure factor) rather than to the structure factor itself. At high temperature this does not cause a serious problem, since the structure factor is flat at high Q, but for the low temperature data (293 K and 490 K) there are still oscillations in this region, making direct transformation unacceptable because of the truncation errors introduced. One way of getting around this is to add to the structure factor an artificial 'tail', which possesses damped oscillations of the same periodicity as those in the high Q region. This proved difficult in the room temperature case, since the radial distribution function was sensitive to details of the 'tail', and so analysis could not be pursued. The 490 K structure factor was treated in this way but the results of the analysis were somewhat anomalous. Even if there is no truncation problem systematic errors from the structure factor are redistributed in an unknown way in the experimental radial distribution function on transformation.

In the present case the problem of the long-range order in crystalline AgBr, or more accurately of the finite configuration size, was tackled in a different way. A cubic simulation with periodic boundary conditions contains real-space information up to length $L/2$, where L is the cube length. Therefore the radial distribution function $g_C^L(r)$ calculated (C) from such a configuration is a section from the actual radial distribution function $g_C^\infty(r)$, calculated by multiplying it by a step function:

$$m(r) = \begin{cases} 1 & \text{if } r \leqslant L/2 \\ 0 & \text{otherwise.} \end{cases} \tag{1}$$

Thus when $g_C^L(r)$ is transformed to reciprocal space the resulting structure factor, $F_C^L(Q)$ is the convolution of $F_C^\infty(Q)$ and the transform of the step function, $m(r)$, that is

$$M(Q) = \sin(QL/2)/Q \tag{2}$$

giving

$$F_C^L(Q_j) = \frac{1}{\pi}\int F_C^\infty(Q_i)\left(\frac{\sin(|Q_i - Q_j|L/2)}{|Q_i - Q_j|} - \frac{\sin(|Q_i + Q_j|L/2)}{|Q_i + Q_j|}\right) \mathrm{d}Q_i. \tag{3}$$

Hence to allow direct comparison with $F_C^L(Q)$, the experimental (E) structure factor $F_E(Q)$ should be convolved with $M(Q)$:

$$F_E^L(Q_j) = \frac{1}{\pi}\int F_E(Q_i)\left(\frac{\sin(|Q_i - Q_j|L/2)}{|Q_i - Q_j|} - \frac{\sin(|Q_i + Q_j|L/2)}{|Q_i + Q_j|}\right) \mathrm{d}Q_i. \tag{4}$$

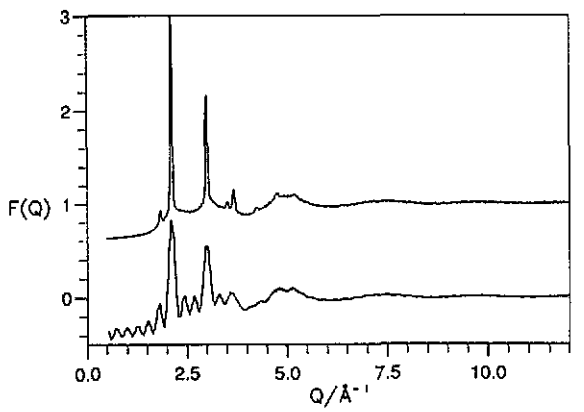

Figure 3. Structure factor, $F_E(Q)$, for AgBr at 699 K, upper solid line (displaced vertically) and comparison between $F_E^L(Q)$, lower solid line and the RMC fit, $F_C^L(Q)$, dashed line. The fit is so good that the dotted line is almost invisible.

If $g_E(r)$ is flat at $r = L/2$, as it would be for many liquids if $L \sim 40$ Å, the convolution does not alter $F_E(Q)$ and is not necessary. Figure 3 shows an example of a structure factor, $F_E(Q)$, and its convolved counterpart, $F_E^L(Q)$. The latter shows

oscillations due to the form of the sinc function with which it has been convolved. The Bragg peaks are lower and broader, because they now represent a finite range in real space (the configuration size, $L/2$). However all information which is contained in a configuration of length L is retained. Intensity lost from the Bragg peaks is redistributed over the rest of Q space. There is no loss of short-range order information, and the long-range order information is retained because of the periodic boundary conditions and the fixed unit-cell size. The philosophy of this approach is essentially the same as Rietveld refinement, where the complete diffraction pattern is fitted as a single entity without attempting to determine the integrated intensities due to individual Bragg peaks. The only difference is that, in this case, the resolution function is related to the model rather than the diffractometer. It should be noted that if one uses RMC to fit to the unconvolved $F_E(Q)$ the fit automatically ends up looking like $F_E^L(Q)$.

Clearly we must also consider the effect of the instrumental resolution function. Ideally the data would be first deconvolved from this, before being convolved with $M(Q)$ to take account of the finite box-size. Alternatively the calculated $F_C^L(Q_j)$ can be convolved with the instrumental function before fitting to $F_E^L(Q_j)$. This introduces errors if the experimental resolution function is not well known. In the present case the full width at half maximum of the main peak of the sinc function is $\Delta Q \sim 0.09\,\text{Å}^{-1}$: the resolution of the diffractometer has this value at about $1\,\text{Å}^{-1}$, increasing to $0.6\,\text{Å}^{-1}$ at $10\,\text{Å}^{-1}$. We must therefore accept that the combination of instrumental resolution and the artificial resolution function of the simulation will result in some increase in the degree of local disorder. However the intention of the present study is to compare local order between different temperatures, rather than to obtain absolute values at any particular temperature. In future we hope to extend the RMC method to simultaneously fit Bragg scattering measured with high resolution and total scattering measured with high statistical accuracy.

4. Results

The trends with temperature in this re-analysis are consistent with those reported in II, but the degree of thermal disorder has been reduced. Very good agreement was obtained between $F_C^L(Q)$ calculated from the RMC model and $F_E^L(Q)$ determined from the experimental measurement (see figure 3), except for our most recent data which could not be accurately corrected (see above). The RMC fit at 293 K was not as good as that obtained for the other temperatures. This is believed to be a consequence of poor background subtraction in the correction procedure, since a slightly different experimental arrangement was used in this case. For this reason the 293 K data are not included in the results presented below.

The mean squared displacement from lattice sites, $\langle u^2 \rangle$, is given as a function of temperature in table 1. This has been calculated directly from the RMC configurations in the manner described in II. The isotropic mean square displacement, which is an average over all directions, is calculated directly from the density of ions in an average unit cell. The mean square displacements along particular directions are determined by considering the averaged ion density along a tube of radius 0.05×lattice constant, centred on the lattice site and pointing in the required direction. The displacements of Br^- ions are isotropic at all temperatures and increase rapidly as the melting point is approached, $\langle u^2 \rangle^{1/2}$ reaching 13% of the lattice spacing at 699 K. The Ag^+ ions

Table 1. The mean square displacements of the ions about their lattice sites ($\langle u^2 \rangle$) in Å^2, and the increase in interstitial (tetrahedral) site occupancy by Ag^+ as a function of temperature up to 699 K. For the Ag^+ separate values are given for mean square displacements in the ⟨100⟩, ⟨110⟩ and ⟨111⟩ directions, as well as an average over all directions (column 2). The mean square displacement of the Br^- is isotropic at all temperatures and so only the average is given. The bracketed numbers give the statistical variation in the last decimal place.

T (K)	Ag^+	Ag^+			Br^-	Ag^+ %
	$\langle u^2 \rangle$	⟨100⟩	⟨110⟩	⟨111⟩	$\langle u^2 \rangle$	interstitials
490±2	0.50 (1)	0.08 (1)	0.08 (1)	0.16 (3)	0.28 (1)	1.7 (3)
669±2	0.93 (1)	0.15 (2)	0.15 (2)	0.29 (5)	0.46 (1)	2.5 (2)
684±2	1.00 (2)	0.19 (2)	0.18 (2)	0.39 (6)	0.50 (1)	2.4 (2)
689±2	1.03 (4)	0.18 (2)	0.17 (2)	0.35 (9)	0.49 (1)	2.5 (3)
697±2	1.10 (4)	0.17 (3)	0.17 (2)	0.38 (5)	0.52 (1)	3.2 (2)
698±2	1.16 (3)	0.19 (3)	0.18 (2)	0.45 (6)	0.55 (1)	3.6 (2)
699±2	1.20 (4)	0.20 (3)	0.19 (3)	0.48 (5)	0.56 (1)	3.9 (4)

have a larger $\langle u^2 \rangle$ than the Br^- ions at all temperatures, but the displacements are anisotropic, by far the greatest being in the ⟨111⟩ direction (see table 1).

Although a large amount of disorder occurs before the melting point, the most recent measurements very close to T_m show that the long range correlations change discontinuously on melting, indicative of a first order transition. The (200) Bragg peak height decreases rapidly in the last degree before melting but still changes discontinuously at T_m, where it completely disappears (see figure 4). To obtain a very approximate value for the rate of change of the mean square displacement with temperature, from the single Bragg peak measurement performed very close to T_m, we assume that the vibrations of both silver and bromine ions are harmonic and isotropic (although this is clearly not the case for the Ag^+). The expression for the (200) peak intensity is:

$$I = I_0(b_{Ag}\exp\{-\tfrac{1}{6}Q^2\langle u^2\rangle_{Ag}\} + b_{Br}\exp\{-\tfrac{1}{6}Q^2\langle u^2\rangle_{Br}\})^2 \qquad (5)$$

where $Q = 2.11$ Å^{-1} and b_x is the scattering length for species x. An estimate of $\mathrm{d}\langle u^2\rangle/\mathrm{d}T$ can only be obtained if one assumes that it is similar for both Ag^+ and Br^-. This is not true in practice (table 1) and the change is thereby under-estimated. With this approximation:

$$\frac{\mathrm{d}I}{\mathrm{d}T} \sim -1.484\frac{\mathrm{d}\langle u^2\rangle_{av}}{\mathrm{d}T}I \qquad (6)$$

where $\langle u^2\rangle_{av}$ is the mean square displacement averaged over Ag^+ and Br^-, giving $\mathrm{d}\langle u^2\rangle_{av}/\mathrm{d}T \sim 0.03$ Å^2 K^{-1} in the last degree before melting, a change of 2.5% per K. This value is of the same order, but smaller, than that calculated from the RMC configurations at slightly lower temperatures (~ 0.035 Å^2 K^{-1} at 3° below T_m from table 1). This is as expected because of the approximations made and the fact that RMC tends to produce structures which are relatively disordered, as discussed earlier.

Figure 5 shows the partial radial distribution function, $g_{Ag\text{-}Ag}(r)$, at various temperatures. It is seen that the main peak in the solid state at $r \sim 4$ Å decreases in height, whilst the peak at $r \sim 2.6$ Å increases, becoming the main peak in the liquid.

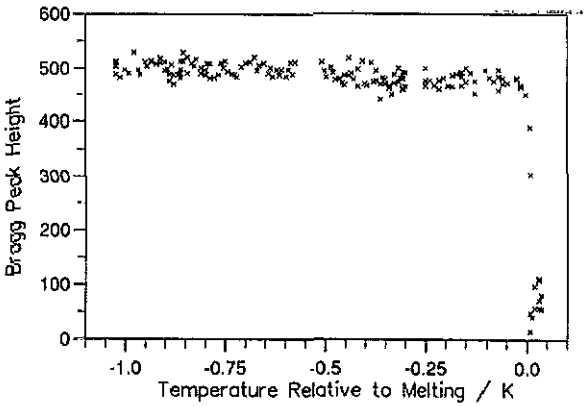

Figure 4. (200) Bragg peak height (arbitrary units), close to the melting point. Measurements were taken every minute during a continuous heating ramp.

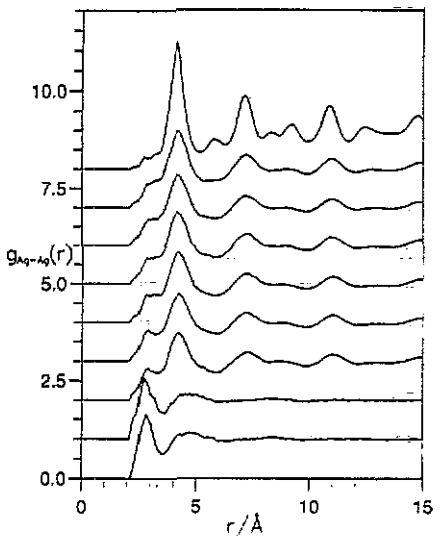

Figure 5. $g_{Ag-Ag}(r)$ at 706, 703, 699, 698, 697, 689, 684, 669 and 490 K. Successive temperatures are displaced vertically by 1.0.

This is close to the distance between lattice site and neighbouring $(\frac{1}{4}\frac{1}{4}\frac{1}{4})$ interstitial position in the crystal, so the development is consistent with an increasing number of Ag^+ occupying the interstitial tetrahedrally coordinated (T) positions as well as the regular octahedral (O) ones. In the crystal the occupancy of T sites can be calculated by considering the actual distribution of silver ions. We define interstitials to be those silver ions within $0.12\times$lattice spacing of the T site (see II for the reasons behind this choice); a rapid increase in their number is found as the melting point is approached (table 1). It should be noted that we probably over-estimate the percentage of interstitials at all temperatures, both because of the criterion we have used to define them and the fact that RMC produces relatively disordered structures. Some Ag^+ which are vibrating about the true lattice sites, rather than about interstitial sites, are included in our summation. The percentage at 490 K probably gives an idea of the size of the error, since there are unlikely to be a significant number of Frenkel defects at

this temperature. However, there is no unambiguous way of defining such thermally induced defects since the density distribution between the lattice and interstitial sites is continuous.

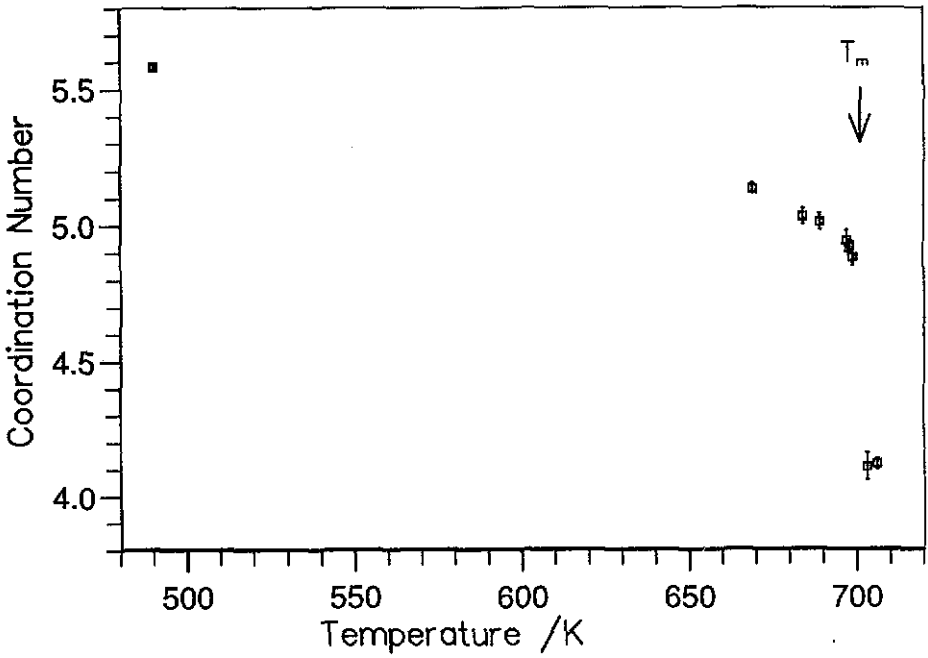

Figure 6. Coordination number for unlike ions, N_{Ag-Br}, as a function of temperature. The melting point, T_m, is indicated. The error bars show the statistical variation between different configurations.

While the number of interstitials is a useful guide to disordering in solid AgBr it is perhaps more useful to look at parameters that can be calculated for both the solid and melt. One such parameter is the first shell coordination number for unlike ions, N_{Ag-Br}. This is calculated from the integral of $g_{Ag-Br}(r)$ up to 3.6 Å, which is close to the first minimum at all temperatures. N_{Ag-Br} equals 4 for perfect T coordination and 6 for perfect O coordination, whereas for a situation in which the 4 Ag^+ in the unit cell occupy the 12 T and O sites of the FCC lattice with equal probability $N_{Ag-Br} \sim 4.6$. These numbers are decreased by thermal vibration. Figure 6 shows the variation of N_{Ag-Br} with temperature. It can be seen that while it decreases more rapidly as T_m is approached there is still a large jump between 699 and 703 K. The value in the liquid just after melting is 4.11 ± 0.05, so that we are in a regime where both O and T positions are occupied. This is confirmed by examination of the bond angle distributions, where a bond is defined as a vector joining two ions which are within a certain radius (chosen as the first minimum in the appropriate $g_{\alpha-\beta}(r)$). This is a purely geometrical definition, no chemical bonding is implied. Figure 7 shows the Ag–Br–Ag and Br–Br–Br distributions at 490, 699 and 703 K. The Br–Br–Br distribution shows no symmetry change with temperature, so the local arrangement of Br^- is not changing unexpectedly. However for Ag–Br–Ag a peak at $\sim$ 55° increases in magnitude as the temperature is raised. This corresponds to a situation where there is both O and T occupation, as indicated in figure 7. It is

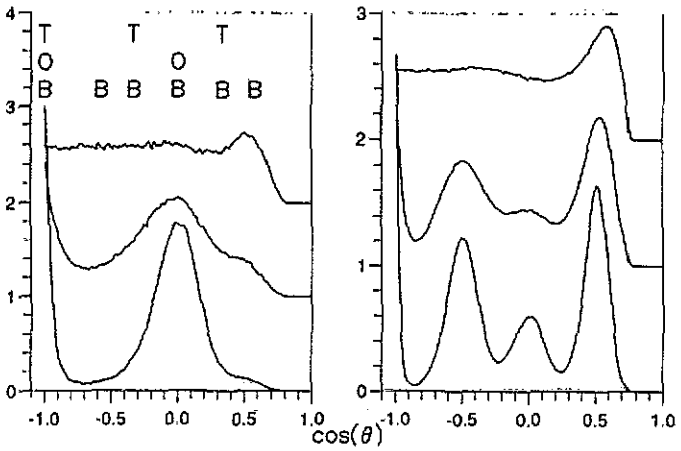

Figure 7. Ag–Br–Ag and Br–Br–Br bond angle distributions at 490, 699 and 703 K (T_m = 701 K). Successive temperatures are displaced vertically by 1.0. Maximum bond-lengths are 3.6 and 5.1 Å for Ag–Br and Br–Br, respectively. The cosines which would be obtained for various perfect FCC crystals are given, where T indicates four Ag^+ randomly occupying the eight tetrahedral sites, O indicates occupation of the four octahedral sites and B random occupation of the T and O sites; in all cases Br^- occupy a perfect FCC sub-lattice.

hardly visible at 490 K, is seen as a shoulder at 699 K and as the major peak in the melt.

5. Discussion

The results show that, while there are increasing numbers of Ag^+ in the T interstitial sites in the solid (up to several percent close to T_m), in the melt there are comparable numbers of Ag^+ ions in O and T positions. For many salts melting does not radically alter the local atomic environment (McGreevy and Pusztai 1990) and so the changes in the silver sub-lattice do not seem consistent with 'pre-melting', where one would expect to see progressive disordering without alteration of the fundamental symmetry. Similarly these changes are not necessarily a precipitating factor for the melting transition, since in other fast-ion conductors (e.g. $SrCl_2$, CuI and CuBr) considerable disorder of one sub-lattice is possible over an extended temperature range in the solid state. We cannot comment on the role played by Schottky defects, suggested by Andreoni and Tosi (1983) to be responsible for the melting process, since these cannot be modelled using the RMC technique. However, they are not necessary to reproduce the data.

We explain the increasing disorder of the Ag^+ sub-lattice as due to the onset of a second-order transition and follow Andreoni and Tosi (1983) in suggesting that, in the absence of melting, the resultant phase would be fast-ion conducting. If the local order of the melt can be taken as representative, the bond angle distributions and N_{Ag-Br} values indicate that in this phase the Ag^+ would be distributed over both T and O sites and able to diffuse between them, the majority of the ions taking part in conduction. For a perfect crystal with FCC Br^- and Ag^+ in the resulting T sites the contributions to the (200) Bragg peak from the two sub-lattices largely cancel, whilst

for Ag^+ in the O positions the contributions are additive. The peak height directly before melting (figure 4) indicates that the Ag^+ are still mostly in the O positions, which implies that the transition temperature would be above T_m. To determine this temperature would require fitting to Bragg peak intensities measured over about 10° below T_m; the data from figure 4 do not cover a sufficient range and are too inaccurate.

A study of AgBr close to the melting point at higher pressures might lend further insight by separating any 'pre-melting' effects from those due to the fast-ion transition, provided the fast-ion phase boundary does not follow the melting curve. This second-order transition might be expected to be similar to the one to fast-ion behaviour in the high-pressure FCC phase of AgI and so a study of this region of the AgI phase diagram would be instructive. However accurate temperature work at high pressures is difficult. The only structural work on fast-ion FCC AgI known by the authors is the constant-stress molecular dynamics calculations of Tallon (1986), in which the structure was found, on quenching, to still be that of rocksalt.

6. Conclusion

We have reported the first use of RMC fitting to structure factor data convolved to take account of the finite model size. The results are consistent with previous work which used RMC to fit radial distribution function data and extend the region of fitting to lower temperatures with greatly improved accuracy. As in previous work a steady increase was found in the number of $(\frac{1}{4}\frac{1}{4}\frac{1}{4})$ Ag^+ tetrahedral interstitials as the melting point is approached. We conclude that the silver ions are undergoing a second-order transition with a critical temperature above the melting point of AgBr. This is the diffuse transition to fast-ion conducting behaviour proposed by Andreoni and Tosi (1983). The final structure, if melting did not intervene, is postulated to be one in which the silver ions would occupy both the octahedral and tetrahedral positions of the FCC bromine sub-lattice and diffuse between them. The increase in conductivity and disorder of the Ag^+ sub-lattice close to the melting point is then largely due to this diffuse transition to fast-ion conducting behaviour, rather than being a 'pre-melting' effect. A similar study of the FCC phase of AgI would be instructive in substantiating this conclusion. The large amount of disorder in the silver sub-lattice does not seem to alter the first order nature of the melting transition.

Acknowledgments

We would like to thank all the staff at the Institut Laue-Langevin, in particular Pierre Convert, for assistance with these experiments. VMN wishes to acknowledge the SERC for the award of a postgraduate studentship during the course of which this work was performed. RLM thanks the Royal Society for continued support.

References

Akella J, Vaidya S N and Kennedy G C 1969 *J. Appl. Phys.* **40** 2800
Andreoni W and Tosi M P 1983 *Solid State Ion.* **11** 49
Boyce J B, Hayes T M, Stutius W and Mikkelsen J C 1977 *Phys. Rev. Lett.* **38** 1362

Devlin B A and Corish J 1987 *J. Phys. C: Solid State Phys.* **20** 705
Hamilton J F 1988 *Adv. Phys.* **37** 359
Keen D A, Hayes W and McGreevy R L 1990a *J. Phys.: Condens. Matt.* **2** 2773
Keen D A, McGreevy R L, Hayes W and Clausen K N 1990b *Phil. Mag. Lett.* **61** 349
Lawn B R 1963 *Acta Crystallogr.* **16** 1163
McGreevy R L, Howe M A, Keen D A and Clausen K N 1990 *IOP Conf. Ser.* ed M W Johnson **107** 165
McGreevy R L and Pusztai L 1988 *Mol. Simul.* **1** 359
—— 1990 *Proc. R. Soc.* A **430** 241
Mellander B-E 1982 *Phys. Rev. B* **26** 5886
Mellander B-E, Bowling J E and Baranowski B 1980 *Phys. Scr.* **22** 541
Metropolis N, Rosenbluth A W, Rosenbluth M N, Teller A H and Teller E 1953 *J. Phys. Chem.* **21** 1087
Tallon J L 1986 *Phys. Rev. Lett.* **57** 2427
Tallon J L and Buckley R G 1983 *Solid State Commun.* **47** 563